A comparison of the fluid factor with λ and μ in AVO analysis

George C Smith, University of Cape Town, and Maurice Gidlow, PGS, Oslo.*

Introduction

Smith and Gidlow (1987) introduced the fluid factor in amplitude versus offset (AVO) analysis. It was designed to be a direct hydrocarbon indicator. Goodway et al. (1997) suggested that Lamé's elastic parameters λ and μ, and their products with density, could be useful tools in AVO analysis. They suggested in particular that λ, or its product with density, λρ, can be a direct hydrocarbon indicator. Gray et al. (1999) gave a method of estimating these parameters more directly, as does Chen (1999).

Castagna and Smith (1994) presented a set of 25 world-wide measurements of P- and S-wave velocities and densities in associated shales, brine-saturated sands and gas-saturated sands and compared various commonly used AVO parameters. They concluded that the indicator Rp - Rs (the difference between P- and S-wave reflectivities) satisfy the conditions desirable for a hydrocarbon indicator. Smith and Sutherland (1996) used these 25 examples to demonstrate the application of the fluid factor, Rp – gRs (where g is a statistically derived gain function), and the improvement obtained compared with the other AVO parameters.

The purpose of this paper is to use Castagna and Smith's (1994) worldwide examples to compare the Lamé parameters with the fluid factor.

Lamé parameters

Lamé's constants are elastic moduli, which have been found useful in the description of the elastic behaviour of materials. The modulus μ is the shear modulus or rigidity, but λ is generally held to have no physical meaning, being a parameter substituted into equations describing elastic behaviour to make them simpler. It can be defined by

$$\lambda = k - \frac{2}{3}\mu$$

where k is the bulk modulus or incompressibility. Poisson's ratio, in terms of Lamé constants, is given by

$$\sigma = \frac{\lambda}{2(\lambda + \mu)}$$

Poisson's ratio generally varies between 0 and ½. A material has a Poisson's ratio of ½ if it increases its cross-sectional area when compressed to the extent that its volume does not change. This limit occurs when μ=0, i.e. the material is a fluid. A material has a Poisson's ratio of 0 if, when unconstrained laterally, it does not increase its cross-sectional area when compressed. This limit occurs when λ=0, and therefore incompressibility, k, is equal to two thirds of rigidity μ. Thus a material can have a certain incompressibility, and no rigidity (a fluid), but it cannot have rigidity and be highly compressible. Rigidity implies a certain minimum incompressibility, and λ can be thought of as the excess incompressibility over that minimum.

Reflectivity equations

The methodology used by Goodway et al (1997) is to extract the compressional reflectivity section ΔI/I and the shear wave reflectivity section ΔJ/J by AVO analysis using the reflectivity equation described by Gidlow et al. (1992) and Fatti et al. (1994), equation (1). I and J are P- and S-wave impedances respectively.

$$R(\theta) = \frac{\Delta I}{2I}\left(1 + \tan^2\theta\right) - 8\frac{J^2}{I^2}\frac{\Delta J}{2J}\sin^2\theta - \frac{\Delta\rho}{2\rho}\left(\tan^2\theta - 4\frac{J^2}{I^2}\sin^2\theta\right) \qquad (1)$$

They then obtain I and J through conventional inversion. λρ and μρ are obtained from the relationships:
$\lambda\rho = I^2 - 2J^2$ and $\mu\rho = J^2$

Using these relationships equation (1) can be transformed into equation (2) (Gray et al., 1999). In equation (2), α and β are P- and S-wave velocities respectively.

$$R(\theta) = \left(\frac{1}{4} - \frac{1}{2}\frac{\beta^2}{\alpha^2}\right)\left(\sec^2\theta\right)\frac{\Delta\lambda}{\lambda} + \left(\frac{\beta^2}{\alpha^2}\right)\left(\frac{1}{2}\sec^2\theta - 2\sin^2\theta\right)\frac{\Delta\mu}{\mu} + \left(\frac{1}{2} - \frac{1}{4}\sec^2\theta\right)\frac{\Delta\rho}{\rho} \qquad (2)$$

In order to minimize the coefficient of Δρ/ρ, equation (2) can be written in terms of L and M, where L= λρ and M = μρ, to give equation (3).

$$R(\theta) = \left(\frac{1}{2} - \frac{J^2}{I^2}\right)\left(\sec^2\theta\right)\frac{\Delta L}{2L} + \left(\frac{J^2}{I^2}\right)\left(\sec^2\theta - 4\sin^2\theta\right)\frac{\Delta M}{2M} - \left(\tan^2\theta - 4\frac{J^2}{I^2}\sin^2\theta\right)\frac{\Delta\rho}{2\rho} \qquad (3)$$

Smith (1999) suggested that ΔL and ΔM be derived directly by applying a gain function proportional to a smoothed I^2 function (I^2 = L + 2M). This is shown in equation (4) below:

$$4I^2 R(\theta) = \Delta(\lambda\rho)\sec^2\theta + 2\Delta(\mu\rho)(\sec^2\theta - 4\sin^2\theta) \qquad (4)$$

Method

It is instructive to examine this data set in the cross-plot domain. Figures 1a and 1b show the data displayed in the J vs. I and M vs. L domains. The separation between gas-sands and non-pay lithologies is clear. And it is this separation which we attempt to quantify in the process of AVO analysis.

A comparison of the fluid factor with λ and μ in AVO analysis

Following the method of analysis of Castagna and Smith (1994), and Smith and Sutherland (1996), the following are compared in Figure 2: a) fluid factor, b) $\Delta L/L$, c) $\Delta L/(L+2M)$, and d) $\Delta J/J$ (or $\frac{1}{2}\Delta M/M$).

For each of the 25 sets of data points (each set consisting of gas/shale, gas/brine, and shale/brine interfaces), the following were computed:

- i) actual values of $\Delta I/I$, $\Delta J/J$, $\Delta L/L$, $\Delta L/(L+2M)$;
- ii) the amplitude variation with angle for each set using the Zoeppritz (1919) equations (0 to 38 degrees);
- iii) least square best-fit estimates of the parameters listed in i) above by fitting equations 1, 3 and 4.

During the curve fitting, the third term (of equations 1 and 3) is omitted because of the instability that occurs in practice when fitting three term equations to less than noise-free data sets.

Results and conclusions

The fluid factor, $\Delta L/L$ and $\Delta L/(L+2M)$ all satisfy the criteria for a desirable hydrocarbon indicator:

- Background (non-pay) is constant and near zero.
- The indicator is generally negative for shale over gas sand
- The indicator is generally positive for gas sand over brine sand
- The indicator will work for any class of sand.

In fact, the values obtained by fitting the equations for $\Delta L/L$ and for $\Delta L/(L+M)$ are, within a scale factor, identical. It will be observed, however, that the actual values are much closer to the fitted values in the case of $\Delta L/(L+M)$ than in the case of $\Delta L/L$. This is because there is an assumption in deriving equation 3 (as in all the others) that the changes in property are small compared with the value of the property. This is not the case for $\lambda\rho$, for in gas sands especially, the values for $\lambda\rho$ can be close to zero, and much lower than the differences in $\lambda\rho$. Samples showing greatest error between actual and fitted values are those with the largest fractional change in $\lambda\rho$ across the interface. It is interesting to note that $\Delta L/(L+M)$ and $\Delta M/(L+M)$ are obtained without making any assumptions about velocity or impedance contrasts.

The values for the fluid factor were obtained from the fitted reflectivities as follows: from the estimates of P-wave and S-wave reflectivities, the scaling factor g was obtained which minimised the fluid factor of the background in an average sense as described in Smith and Sutherland (1996).

It will be observed that the fluid factor values so derived are very similar to the fitted values for $\Delta L/(L+2M)$ as well. The difference is only because in the fluid factor approach there is freedom to choose the scalar g to optimise the result, while in the $\lambda\rho$ approach the scalar is effectively fixed.

Our expectation that shear reflectivity is dependent upon lithology rather than pore fluid is confirmed in Figure 2d. The shale/brine sand and shale/gas sand exhibit significant (and similar) reflectivities compared with the case of gas sand/brine sand.

It can be concluded that there is a great deal of equivalence between fluid factor analysis and λ, μ, ρ analysis, and each can give insight into the meaning of the other. We believe that the extra flexibility involved in the fluid factor approach, makes it a more appropriate tool in practical AVO analysis.

References

Castagna, J. P. and Smith, S. W., 1994, Comparison of AVO indicators: a modelling study: Geophysics, 59, 1849-1855.

Chen, X. C., 1999, Essentials of Geomodulus Method, 1999 SEG Expanded Abstracts.

Fatti, J. L., Vail, P. J., Smith, G. C., Strauss, P. J. and Levitt, P. R., 1994, Detection of gas in sandstone reservoirs using AVO analysis: A 3-D seismic case history using the geostack technique: Geophysics, 59, 1362-1376.

Gidlow, P.M., Smith, G.C., and Vail, P.J., 1992, Hydrocarbon detection using fluid factor traces: A case history, Expanded abstracts of the Joint SEG/EAEG Summer Research Workshop on "How useful is Amplitude- Versus Offset (AVO) Analysis?": 78-89

Goodway, W., Chen, T., and Downton, J., 1997, Improved AVO fluid detection and lithology discrimination using Lamé petrophysical Parameters; "Lambda-Rho", "Mu-Rho", & "Lambda/Mu fluid stack", from P and S inversions: 1997 CSEG meeting abstracts, 148-151:1997 SEG meeting abstracts, 183-186.

Gray, D., Goodway, W. and Chen, T, 1999, Bridging the gap: Using AVO to detect changes in fundamental elastic constants: 1999 SEG meeting abstracts, 852-855.

Smith, G. C., 1999, The relationship between Lamé's constants, lambda and mu, and the fluid factor in AVO analysis of seismic data: South African Geophysical Association meeting abstracts, 6.3.

Smith, G. C. and Gidlow, P. M., 1987, Weighted stacking for rock property estimation and detection of gas: Geophys. Prosp., 35, no. 09, 993-1014.

Smith, G. C. and Sutherland, R. A., 1996, Short note – The fluid factor as an AVO indicator: Geophysics, 61, no. 05, 1425-1428.

Zoeppritz, K., 1919, Erdbebenwellen VIII B, Uber Reflexion und Durchgang seismischer Wellen durch Unstetigkeitsflachen: Gottinger Nachr., 1, 66-84.

a) S-wave impedance vs. P-wave impedance.

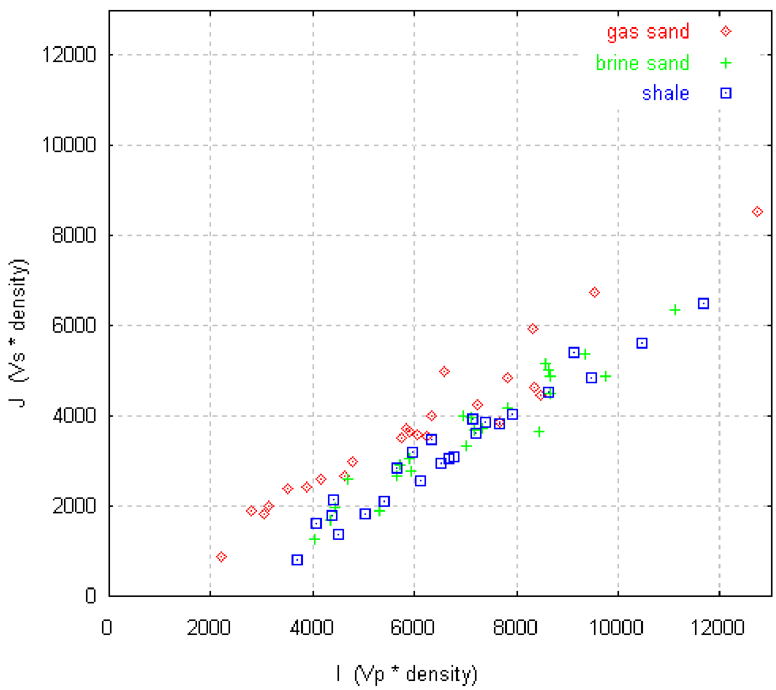

b) μρ vs. λρ

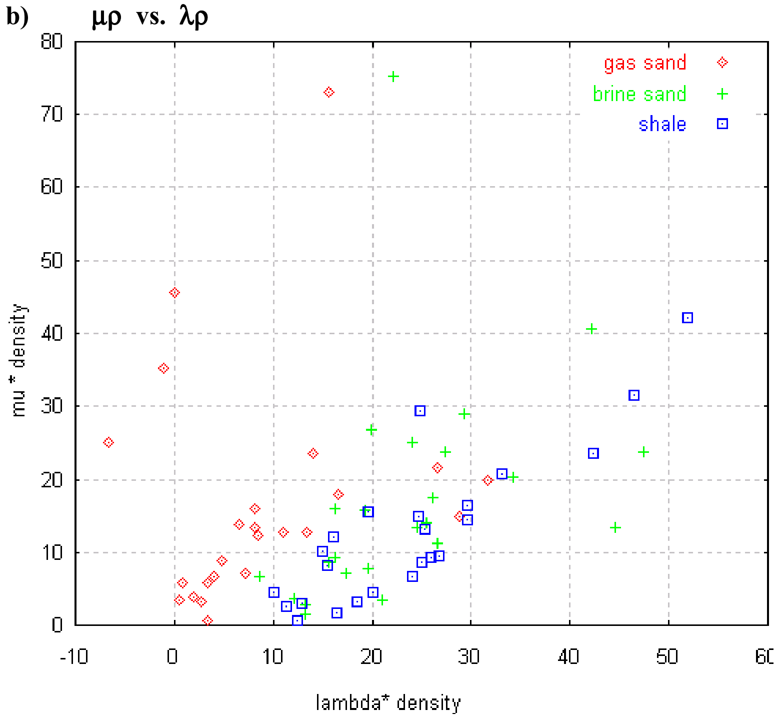

Figure 1. Cross-plot domain representation of 25 shale/ brine sand, shale/gas sand, and gas sand/brine- sand.sets a) J vs I (S-wave impedance vs. P-wave impedance) b) μρ vs. λρ

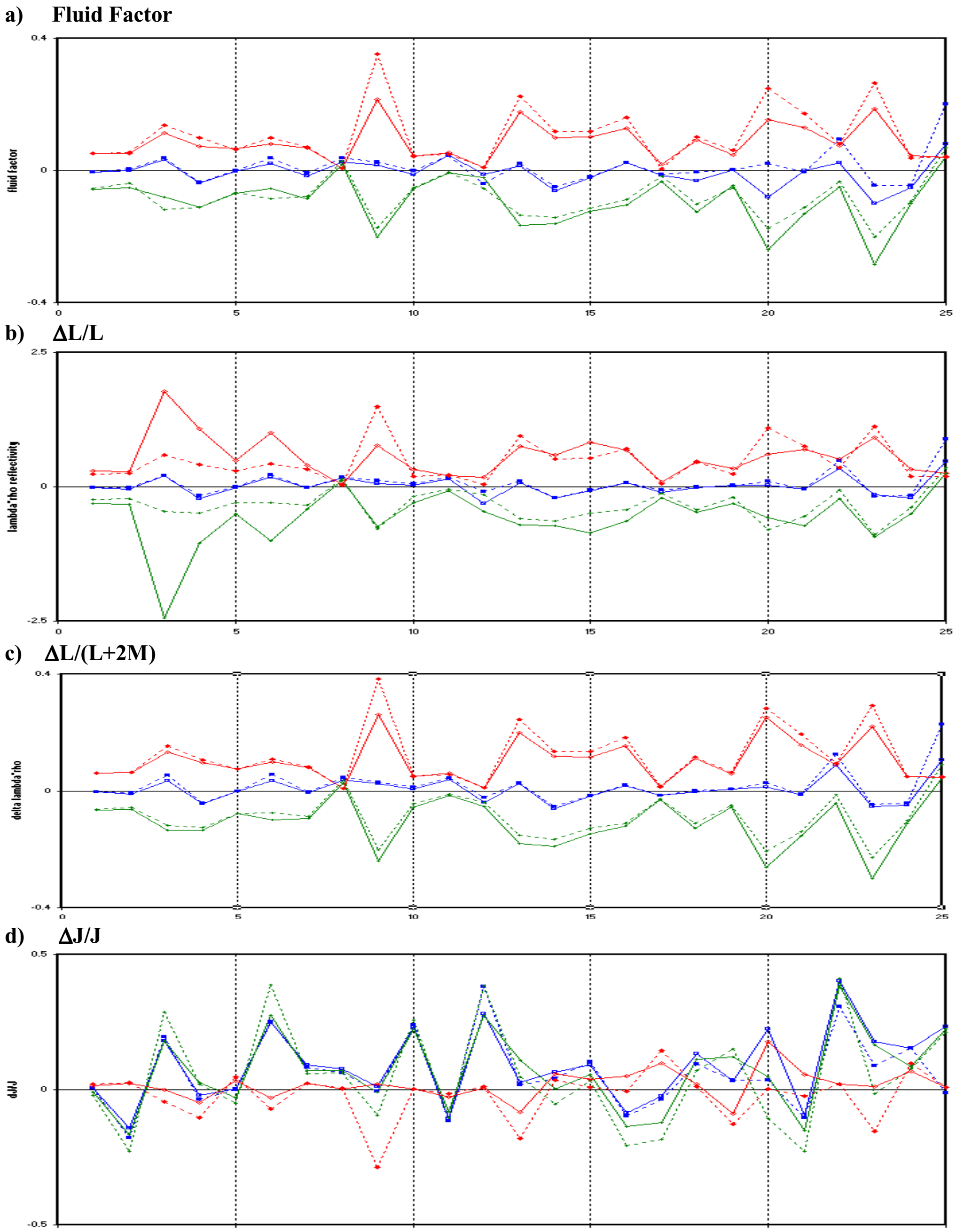

Figure 2: a) Fluid factor, b) ΔL/L, c) ΔL/(L+2M), and d) ΔJ/J for the interfaces shale/ brine sand, shale/gas sand, and gas sand/brine sand. Solid lines correspond to computed values; the dotted lines correspond to least square best-fit estimates of the curves described by equations (1), (3) and (4).

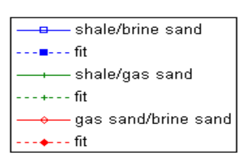

A comparison of the fluid factor with λ and μ in AVO analysis